Reelin expression is up-regulated in mice colon in response to acute colitis and provides resistance against colitis

Ana E. Carvajal, María D. Vázquez-Carretero, Pablo García-Miranda, María J. Peral, María L. Calonge* and Anunciación A. Ilundain

Department of Physiology, University of Seville, Spain

Abbreviations: α-SMA, α-smooth muscle actin; ApoER2, apolipoprotein E receptor 2; CASK, calcium/calmodulin-dependent serine protein kinase; Dab1, Disabled-1; DSS, dextran sulphate sodium; DNMT1, (DNA (Cytosine-5-)-Methyltransferase 1); IL-1β, interleukin-1β; PDGF-BB, platelet derived growth factor β; TGF-β1, transforming growth factor β1; TNF-α, tumour necrosis factor α; Sp1, transcription factor Sp1, Tbr1, T-box brain 1; VLDLR, very low-density lipoprotein receptor;

* Correspondence to Dr. M.L. Calonge
Dpto. Fisiología
Facultad de Farmacia
C/ Profesor García González, nº 2
41012, Sevilla, Spain
Phone: 34 954556388
E mail: calonge@us.es

Abstract

Studies on the reelin signalling system in rodent small intestine suggest that the system protects the organism from intestinal pathology. The expression of the reelin signalling system, determined by real time-PCR and immunological assays, its response to dextran sulphate sodium (DSS) and the response of wild-type and reeler mice to DSS have been determined in the colon. DNA methylation was determined by bisulfite modification and sequencing of genomic DNA. Reelin expression in the colon mucosa is restricted to the myofibroblasts, whereas both epithelial cells and myofibroblasts express its receptors (ApoER2 and VLDLR) and its effector protein Dab1. Reelin protein is also detected within the muscle layer. DSS-treatment reduces reelin expression in the muscle layer but its expression is activated in the mucosa. Activation of mucosal reelin is greater in magnitude and is delayed until after the activation of the myofibroblasts marker, α-SMA. This indicates that the DSS-induced reelin up-regulation results from changes in the reelin gene expression rather than from myofibroblasts proliferation. DSS-treatment does not modify Sp1 or Tbr1 mRNA abundance, but increases that of TGF-β1 and ApoER2, decreases that of CASK and DNMT1 and also decreases the methylation of the reelin promoter region. Finally, the reeler mice exhibited higher inflammatory scores as compared with wild-type mice, indicating that the mutation increased the susceptibility to DSS-colitis. We conclude that the myofibroblasts of mouse distal colon increase the production of reelin in response to DSS-colitis by a DNMT1-dependent hypo-methylation of the gene promoter region and that reelin provides protection against colitis.

Keywords: reelin, colon, DSS-colitis, DNMT1

1. Introduction

The epithelium of the mammalian intestine is a highly differentiated single cell layer that constitutes both, a physical and functional barrier between the external environment and the organism. To preserve cellular integrity and tissue homeostasis, the intestine self-renews every 3 to 6 days by continuous cell renewal originating from stem cells, located at the crypts, which produce transient amplifying cells. In the colon epithelium the transient amplifying cells give rise to three differentiated cell types: colonocytes, goblet cells and enteroendocrine cells. These cell types differentiate while migrating up to the surface epithelium. Colonocytes have absorptive and secretory functions, goblet cells produce mucins that protect the mucosa from injury and enteroendocrine cells secrete hormones that regulate gastrointestinal function. In contrast to the small intestine, the colon lacks Paneth cells, has larger crypts and, instead of villi, it has a rather flattened surface epithelium facing the lumen [1].

The homeostasis of the intestinal epithelium is based on the balance between cell proliferation, differentiation and apoptosis. In the embryo and in the postnatal animal, the regulation of the intestinal epithelium growth and differentiation depends on bidirectional signals between the epithelium and mesenchymal cells. This is particularly relevant to the intestinal myofibroblasts, located immediately subjacent to the epithelial cells basement membrane. These cells are considered to orchestrate diverse intestinal events, such as the control of epithelial turnover, tissue repair, inflammation and the immune response. The myofibroblasts fulfill all these functions by expressing and secreting various extracellular matrix components (cytokines, growth factors, inflammatory mediators, adhesion proteins, among others), as well as expressing receptors for many of these ligands, thereby permitting bidirectional information flow between the intestinal epithelium and the extracellular matrix (see [2,3] for reviews).

We have reported that rodent small intestine [4,5] and human colon [6] express reelin; its receptors apolipoprotein E receptor 2 (ApoER2) and very low density lipoprotein receptor (VLDLR), and its effector protein disabled-1 (Dab1) [4]. Within the mucosa reelin expression is restricted to the myofibroblasts whereas the other proteins are expressed by both, myofibroblasts and epithelial cells [4–6]. We also found that the absence of reelin (*reeler* mutation) modifies the small intestine morphology and

decreases epithelial cell proliferation, migration and apoptosis, both in the suckling and adult mice [5,7]. Wild type and reeler mice display a range of aberrant phenotypes including reduced number of Paneth cells, expanded intercellular space of the adherens junctions and desmosomes, and increased gene expression related to pathological immune response, inflammation and tumour development. These findings prompted us to consider that reelin may have a role in pathological conditions [5,7].

The purpose of the current work was to: i) study the expression of the reelin signalling system in the colon, ii) test whether the system is affected by dextran sulphate sodium (DSS)-induced colitis and iv) find out whether reelin protects the organism from the development of colitis.

Preliminary reports of some of these results were published as abstracts [8–10].

2. Materials and methods

2.1. Materials

The antibodies used for immunocytochemistry were: rabbit anti-reelin G10 from Novus Biologicals Europe, Cambridge, UK; rabbit anti-reelin (sc5578), rabbit anti-ApoER2 (sc20746) and mouse anti-VLDLR (sc18824), from Santa Cruz Biotechnology, Inc., Santa Cruz, CA, Dallas, TX, USA; mouse anti-α-smooth muscle actin (α-SMA) (A5228) from Sigma-Aldrich, Madrid, Spain; rabbit anti-Dab1 (AB5840) from Chemicon, Temecula, CA, USA; Biotin-conjugated anti-mouse and anti-rabbit IgG were obtained from Vector Laboratories Inc. CA, USA; FITC-conjugated anti-rabbit or anti-mouse IgG from Jackson Immuno Research Laboratories, Inc. Baltimore, USA and Alexa Fluor 546 anti-mouse IgG from Thermo Fisher Scientific, IL, USA. The antibodies employed for Western Blot assays were: rabbit anti-reelin G10 from Novus Biologicals; mouse anti-α-SMA (A5228), mouse anti-β-actin (A5316), mouse anti-GADPH (G8795) and rabbit anti-DNMT1 (DNA (Cytosine-5-)-Methyltransferase 1) (D4692) from Sigma-Aldrich, Madrid, Spain. Peroxidase-conjugated anti-mouse and anti-rabbit IgG were obtained from Sigma-Aldrich, Madrid, Spain. Unless otherwise stated, the other reagents used in the current study were from Sigma-Aldrich.

2.2. Animals and experimental conditions

Sixteen day-old, 1 and 3 month-old C57BL/6 mice and 3 month-old B6C3Fe control and *reeler* (rl^-/rl^-) mice were used. *Reeler* mice were purchased from Jackson Laboratories through Charles River Laboratories. The animals were housed in a 12:12 light–dark cycle and fed *ad libitum* with either a Global rodent diet for C56BL/6 mice or Global 2019 extruded rodent diet for B6C3Fe mice (Harlan Iberica S.L.), with free access to tap water. *Reeler* mice were genotyped by polymerase chain reaction (PCR) analysis of genomic DNA using the primers (5´-3´) TAATCTGTCCTCACTCTGCC, CAGTTGACATACCTTAAT and TGCATTAATGTGCAGTGT [11]. The animals were humanely handled and sacrificed by cervical dislocation, in accordance with the European Council legislation 2010/63/EU concerning the protection of experimental animals.

The dextran sulphate sodium (DSS, MW 40 KDa; TdB Consultancy) colitis model was employed because it produces many of the events presumed to initiate and sustain human intestinal bowel diseases. Three month-old C57BL/6 mice, of similar body

weight values, were randomized into untreated (control) and DSS-treated groups, which received either water or water containing 3% (wt/vol) DSS, respectively. Daily, throughout the DSS-treatment, two observers recorded body weight, stool consistency and presence of blood in faeces. A score (scale of 0-3) was assigned to each of these parameters and the three variables were averaged at each time to calculate the average daily disease activity index (DAI) as described by Cooper et al. [12]. Animals were sacrificed at day 9 of treatment, the time at which the loss of body weight is about 10 % of the initial weight. In some experiments mice were sacrificed at 0, 3, 6 or 9 days after initiation of DSS-treatment.

Following sacrifice, the murine intestine was removed, opened longitudinally, washed with ice-cold saline solution and subdivided into the desired intestinal regions. When required, mucosa and muscle layer were separated by scraping. The tissues were either fixed in 4% para-formaldehyde in PBS for histological analysis, frozen at -20ºC for measurements of myeloperoxidase (MPO) activity or frozen at -80ºC for RT-PCR and Western assays.

2.3. Isolation of colonocytes and myofibroblasts

Colonocytes and mucosal myofibroblasts were obtained as previously described [4]. Briefly, intestinal segments were incubated for 15 minutes at room temperature in phosphate-buffered saline (PBS) buffer (in mM: 140 NaCl, 2.7 KCl, 10 phosphate, pH 7.4) (Bioline, #Bio37107) containing 1mM dithiothreitol, followed by a 30 minutes incubation period at 37ºC in PBS buffer containing 1 mM EDTA and 2 mM glucose. After incubation, the tissues were vortexed for 30 seconds and the loosened colonocytes were filtered through a 60 nm nylon textile and collected by centrifugation and resuspended in PBS. For myofibroblasts isolation, the remaining tissue was rinsed with PBS and incubated for 30 minutes in a shaking water bath, at 37ºC, in PBS containing 1 mg/mL collagenase and 2 mg/mL hyaluronidase. The tissues were vortexed for 30 seconds and the myofibroblasts were pelleted and resuspended in PBS. The isolated cells were immediately used for immunostaining.

2.4. Relative quantification of real-time PCR

Total RNA was extracted from the indicated tissue using RNeasy® kit (Qiagen) and sample purity was assessed by spectrophotometric measurement of $OD_{260/280}$. RNA

integrity was analysed by visual inspection after electrophoresis on agarose gel in the presence of ethidium bromide. cDNA was synthesized from 1 µg of total RNA using QuantiTect® reverse transcription kit (Qiagen) as described by the manufacturer. The primers for the genes tested (see Table 1) were chosen according to the mouse cDNA sequences entered in Genbank and designed using PerlPrimer program v1.1.14 (Parkville, Vic., Australia). Real-time PCR was performed with 10 µl Sso Fast™ EvaGreen Supermix (BioRad), 0.4 µM primers and 1 µl cDNA. Controls were carried out without cDNA. Amplification was run in a MiniOpticon™ System (BioRad) thermal cycler (94 °C /3 min; 35 cycles of 94 °C /40 s, 58 °C/ 40 s and 72 °C /40 s, and 72 °C /2 min). Following amplification, a melting curve analysis was performed by heating the reactions from 65 to 95 °C in 1 °C intervals while monitoring fluorescence. Analysis confirmed a single PCR product at the predicted melting temperature. The PCR primers efficiencies ranged from 90 to 110%. The cycle at which each sample crossed a fluorescence threshold, Ct, was determined and the triplicate values for each cDNA were averaged. Analyses of real-time PCR were done using the comparative Ct method, with the Gene Expression Macro software supplied by BioRad. β-actin served as reference gene and was used for samples normalization. The $2^{-\Delta\Delta C'_T}$ method [13] was used to validate β-actin as internal control gene.

2.5. Immunostaining analysis

The cell localization of reelin, Dab1, VLDLR, ApoER2 and α-SMA proteins was performed by immunostaining assays on either intact tissues or isolated cells as previously described by García-Miranda et al. [4]. When intact tissues were used, 7 µm thick cryosections of colon samples were cut and applied to adhesive-coated glass slides. The slides were washed with PBS, permeabilized with 1% Triton X-100 for 15 minutes and washed in PBS for 5 minutes three times. The sections were blocked with 5% bovine serum albumin (BSA), 3% fetal calf serum (FCS) in PBS for 1 h and incubated overnight at 4 °C with the indicated commercial primary antibodies. Antibodies were diluted in PBS containing 5% BSA and 3% FCS. Controls were carried out without primary antibody. Antibody binding was visualized with FITC-conjugated either anti-rabbit IgG or anti-mouse IgG and with Alexa Fluor 546 anti-mouse IgG. Nuclei were visualized with Hoechst 33258. The slides were mounted and photographed with an Olympus BX61 microscope equipped with an Olympus DP73

camera. Images were acquired and analysed by using CellSens Software (Olympus Corporation, Hamburg, Germany).

Isolated colonocytes and myofibroblasts were loaded onto adhesive-coated glass slides, left to dry for 10 minutes at room temperature and fixed with 2% paraformaldehyde in PBS for 10 minutes. The slides containing the isolated cells were washed with PBS, permeabilized with 0.1% Triton X-100 for 20 minutes, washed again and incubated with the desired primary antibody at 4ºC overnight. Antibody binding was visualized with biotinylated secondary antibodies, followed by immunoperoxidase staining using the Vectastain ABC peroxidase kit (Vector) and 3,3'-diaminobenzidine. The slides were mounted and photographed with a Zeiss Axioskop 40 microscope equipped with a SPOT Insight V 3.5.4.1 digital camera (Diagnostic Instrument, Inc.). Acquired images were analysed by using Spot Advance 3.5.4.1 Program analysis (Diagnostic Instrument, Inc).

Controls were carried out without primary antibody.

2.6. Western blot assays

SDS-PAGE was performed on a: i) 4-15% gradient precast polyacrylamide gel (BioRad) for reelin, ii) 7.5% polyacrilamide gel for DNMT-1 and iii) 12% polyacrilamide gel for α-SMA. The lysis buffer contained: 150 mM NaCl, 2 mM EDTA, 10 mM EGTA, 1% NP-40, 0.1% sodium deoxycholate, 1 mM phenylmethylsulfonyl fluoride, 20 µg/ml aprotinin, 10 µg/ml leupeptin and 50 mM Tris-HCl, pH 7.5. Protein was extracted from the desired tissue as described [5]. Briefly, the tissue samples were homogenized in lysis buffer, using a polytron homogenizer, and incubated at 4ºC for 10 minutes on a rotating shaker, followed by centrifugation at 14,000 g for 30 minutes. The resultant supernatant was dissolved in the Laemmli sample buffer. A total of 50µg protein were loaded to each lane, electrophoresed, electrotransferred onto a nitrocellulose membrane and the immunoreactive bands were viewed using a chemiluminescence procedure (GE Healthcare Select®). Anti-β-actin and anti-GAPDH antibodies were used to normalize band density values. Anti-GAPDH was used in the α-SMA Western blot because both proteins have similar MW. The relative abundance of the bands was quantified using the Image J program version 1.46 (National Institutes for Health, http://rsb.info.nih.gov/ij/index.html). Protein was measured by the Bradford method [14] using gamma globulin as the standard.

2.7. Histological assessment of DSS-induced colitis

Histological analysis was performed on 3-4 samples of the distal and proximal colon of each animal to evaluate the grade of inflammation. 5 µm paraffin embedded sections of colon were stained with hematoxylin-eosin [15] and the histological evaluations were performed in a blinded fashion by a validated method described by Cooper et al. [12] with some modifications. The parameters scored on a 0-3 scale were: destruction of epithelium and glands, dilatation of glandular crypts, depletion and loss of Goblet cells, infiltration of inflammatory cells, edema and crypt abscesses.

2.8. Analysis of neutrophil myeloperoxidase activity (MPO)

The enzyme MPO (EC 1.11.1.7) is mostly present in neutrophils and its tissue activity correlates with the quantity of neutrophil infiltration into the tissue. The MPO assay was performed using the o-dianisidine dihydrochloride method as described by Krawisz et al. [16]. Briefly, the proximal and distal colon were homogenized in a buffer containing: 0.5% hexadecyltrimethylammonium bromide, 0.2 M Tris, pH 6, with an Ystral polytron homogenizer (position 5, 30 s x 3, 4ºC) and then subjected to five cycles of freezing and thawing and further disrupted by three sonications (1s/10 pulses). The sample was then centrifuged (7,000 x g, 10 min, 4°C) and the supernatant was used for the MPO assay. 50 µl of either supernatant or MPO standard were added to 150 µl of reaction buffer containing 0.0005% H_2O_2, 0.7 mg/mL o-dianisidine hydrochloride and 50 mM sodium phosphate. The mixture was incubated at 37°C for 5 minutes and the absorbance was measured at 450 nm. One unit of MPO activity was defined as that degrading 1 mmol/min of H_2O_2. The results are expressed as MPO units/mg protein x min. Protein was determined by the method of Bradford [14].

2.9. Bisulfite modification and sequencing of genomic DNA

This assay is based on the conversion of non-methylated cytosine to uracil through bisulfite action, while methylated cytosine remains unaltered. The procedure was performed according to Patterson et al. [17]. Briefly, genomic DNA was isolated from distal colon of control and DSS-treated mice using the commercial Kit “DNeasy® Blood and Tissue” (Quiagen) and DNA yield was estimated by optical density

measurements ($OD_{260/280}$). The DNA was bisulfite-modified with a commercial kit (EZ DNA Methylation™, Zymo Research) and the sequence of reelin promoter region that binds to DNMT1 [18] was subjected to PCR-amplification, using bisulfite specific PCR primer designed using the Methyl Primer Express Software v.1.0 (Applied Biosystem, USA) (5´-GTGATAGTGGTTATGTATGATATGTAG-3´ and 5´-ACCTTCTTAAAACCCCTAAC-3´). Amplification was run in a MiniOpticon™ System (BioRad) thermal cycler (95 °C /1 min; 40 cycles of 95 °C /15 s, 61 °C/15 s and 72 °C /30 s, and 72 °C /5 min). The product was gel-purified, the DNA extracted with a commercial kit "QIAquick® Gel Extraction" (Quiagen) and sequenced by the Genomics and Sequencing Service (IBIS, Sevilla, Spain).

2.10. Statistical analysis

Data are presented as mean ± SEM. In the Figures, the vertical bars that represent the SEM are absent when they are less than symbol height. Comparisons between different experimental groups were evaluated by the two-tailed Student's t-test. One-way ANOVA followed by the Newman-Keuls´test was used for multiple comparisons (GraphPad Prism program). Differences were set to be significant for $p<0.05$.

3. Results

3.1. mRNA levels of reelin and Dab1 in the mice colon

The experimental work was initiated by determining the presence of reelin and its effector protein Dab1 in the colon and by comparing this expression with that in the small intestine. The mRNA levels were evaluated by real time RT-PCR using total RNA isolated from the small and large intestine of 3 month-old mice. Figure 1 shows that the reelin mRNA levels along the small intestine and colon are of the same order of magnitude whereas those of Dab1 decrease from the proximal to distal intestine by approx. two orders of magnitude.

The results in Figure 2 show that in both, proximal and distal colon the maximal levels of reelin mRNA are found at 16 days after birth, whereas no significant differences are observed between 1 and 3 months of life. Dab1 mRNA levels do not change significantly with age and, as described above, the levels are significantly lower in the distal than in the proximal colon at all the ages tested.

3.2. Reelin, Dab1, VLDLR and ApoER2 protein

The cell location of the reelin-Dab1 signalling system in the mice colon was determined by immunostaining assays, on intact tissues and on isolated cells, using antibodies against reelin, Dab1, VLDLR, ApoER2 and α-SMA. α-SMA was used as a myofibroblasts marker. Figure 3 reveals that within the mucosa only the cells expressing α-SMA, namely the myofibroblasts, present a strong reelin-specific staining. The specific signal produced either by the anti-Dab1, the anti-VLDLR or the anti-ApoER2 antibody is seen in colonocytes and myofibroblasts. In the isolated colonocytes, the specific staining of these three proteins is observed in the cytosol, being particularly strong at the cell apical domain. Specific labelling was not detected in the absence of the corresponding primary antibody

3.3. Reelin-Dab1 signalling system in the colon of control and DSS-treated mice

To test whether reelin plays a role under inflammatory conditions we determined the effect of colon inflammation on the expression of the reelin signalling system in the colon. DSS-induced inflammation and the evaluation of the inflammation indicators were performed as described in the Methods. The results summarized in Figure 4 reveal that

the DSS-treatment produced significant changes in the inflammation indicators tested. As compared to control, the DSS-treated mice present a significant increase in: i) the DAI, the colon weight/length ratio, the colon myeloperoxidase activity and the mRNA levels of the pro-inflammatory cytokines IL-1β and TNF-α, ii) a significant decrease in the colon length, iii) a loss of crypt architecture and overall structure of the lamina propria, iv) a massive infiltration of mixed inflammatory cells in the mucosa and submucosa, v) mucosal ulceration and vi) muscle layers thickening.

The effects of DSS-induced colitis on the reelin signalling system were evaluated by measuring the mRNA levels of reelin, Dab1, VLDLR, ApoER2 and of the myofibroblasts marker α-SMA in the proximal and distal colon. The results are given in Figure 5 as the ratio of the mRNA levels measured in the DSS-treated animals *vs*. those measured in untreated mice. They reveal that DSS-treatment significantly augments the mRNA abundance of all the genes under study with the only exception of VLDLR that does not change during inflammation. The DSS-treatment increases reelin mRNA levels by a factor of 4 ± 1 (n=10) and of 11 ± 1 (n=10) in the proximal and distal colon, respectively and these increments are bigger than those of α-SMA mRNA levels (1.8 ± 0.7, n=10 and 2.1 ± 0.5, n=10 in the proximal and distal colon, respectively). These findings indicate that DSS-treatment up-regulates the reelin signalling system. In addition, these results suggest that the reelin up-regulation results from activation of reelin gene expression rather than from an increase in the number of cells expressing reelin and α-SMA, that is of myofibroblasts.

The DSS-induced changes in the markers for inflammation and the mRNA abundance of the genes under study are higher in the distal than in the proximal colon. Because of these observations, the distal colon tissue was used in the rest of the experiments described in the current work.

3.4. Reelin and α-SMA expression vs. duration of the DSS-treatment

To corroborate that the DSS-induced increase in the reelin mRNA levels is independent of the number of myofibroblasts, we measured reelin and α-SMA genes expression in the distal colon of mice treated with 3% DSS in the drinking water during either 0, 3, 6 or 9 days. The DAI, the histological score of the distal colon and the mRNA levels of IL-1β and TNF-α were measured to determine colitis development. Figure 6 shows that distal colon presents a significant increase in inflammation after 3 days of treatment that gradually elevates during the DSS administration. Figure 6 also indicates

that reelin mRNA abundance increases with the duration of the DSS-treatment, as do IL-1β and TNF-α mRNA expression. But, α-SMA mRNA reached maximal mRNA expression levels after three days of DSS treatment and the increment is lower than that observed for reelin mRNA abundance.

To determine whether the DSS-induced increase in reelin gene transcription leads to an increase in reelin protein, we performed Western blot assays on protein extracted from either intact distal colon, mucosa or muscle layer of untreated and of 0, 3, 6 and 9 days DSS-treated mice. The colon of reeler mice was used to verify the specificity of the anti-reelin antibody employed and α-SMA protein abundance was evaluated for comparisons. The results (Figure 7) reveal that the main band detected by the anti-reelin antibody, which is absent from the reeler distal colon, has an apparent molecular mass of approximately 420 kDa, that corresponds to the full-length reelin. Under control conditions (0 days of treatment), the reelin protein abundance is higher in muscle than in the mucosa. DSS increases the abundance of full-length reelin in the mucosa and, as observed with the reelin mRNA levels, the magnitude of the change increases with the duration of the DSS-treatment. The opposite is observed in the muscle layer: the abundance of the reelin protein decreases with the duration of the DSS-treatment. α-SMA protein abundance also increases in the mucosa of DSS-treated mice, but the increase is independent of the duration of the treatment and is lower than that of reelin. Together the observations indicate that the DSS-related increase in α-SMA happens earlier and is lower than the maximum increase in reelin expression, corroborating the view that the DSS-colitis activates reelin gene expression.

3.5. DSS-treatment and the control of reelin expression

To explore the mechanism(s) by which colon inflammation up-regulates reelin gene expression, we evaluated the distal colon of control and DSS-treated mice for: i) the expression of regulators for reelin transcription such as CASK, Sp1 and Tbr1; ii) the expression of the tissue growth factors TGF-β1 and PDGF-BB reported to affect myofibroblasts processes and iii) the expression of DNMT1. The results are given in Figure 8 and include the ApoER2 mRNA values represented in Figure 5 as fold change. It can be seen that DSS-treatment significantly: i) increases the mRNA levels of TGF-β1 and PDGF-BB, ii) decreases those of CASK and DNMT1 and iii) does not modify those of Sp1. The Western blot assay of DNMT1 shows that DSS-treatment also reduces

DNMT1 protein abundance (Figure 8B). Trb1 mRNA is not detected in the mice distal colon by RT-PCR.

Since DSS-treatment decreases DNMT1 expression, we next determined whether the reelin up-regulation involves changes in the methylation of the reelin promoter region. For that we measured the bisulfite modification of -201 to -400 bp sequence of the reelin promoter region, as described in Methods. The results (Figure 9) reveal that the reelin promoter region examined presents thirty 5´CpG dinucleotides and that twenty two of them are significantly down-methylated by the DSS-treatment.

These findings indicate that the DSS-induced decrease in DNMT1 expression leads to hypo-methylation of the reelin gene promoter region and that other factors might also regulate reelin gene transcription.

Effect of the DSS on the colon of wild-type and reeler mice

To find out whether reelin protects the organism from the development of colon pathology, such as acute colitis, we compare the response of wild-type and reeler mice to DSS-induced colitis. Wild-type and reeler mice were subjected for 9 days to DSS treatment and clinical and histological characterization of the colon were used to assess colitis severity, as described in Methods. The results given in the Figure 10 reveal that the reeler mice developed a more severe colitis than wild-type mice, because the reeler mice exhibit higher: i) mortality during the DSS treatment (40% *vs.* 10% in wild-type mice) and ii) inflammatory parameters score (DAI, colon weight/length ratio, MPO activity, IL-1β □□□□ levels and histological scores). All these results indicate that the reeler mutation increases the susceptibility to DSS-induced inflammation.

4. Discussion

Ulcerative colitis is a complex disease in which genetic and environmental factors interact to promote a detrimental immune response in the gut and imbalance between pro-inflammatory and anti-inflammatory reactivity. The anti-inflammatory reactivity determines whether the immune response to gut antigens is detrimental or innocuous. Herein we show that the reelin signalling system is present in the colon, it is up-regulated by experimental colitis and it might have an anti-inflammatory action.

The expression of the reelin signalling system in the mice colon resembles that previously observed in rodent small intestine [4,5] and human colon [6] in that: i) the mucosal myofibroblasts produce reelin and ii) as reelin receptors and Dab1 are expressed by both, epithelial cells and myofibroblasts, reelin might have paracrine actions on the epithelial cells and autocrine actions on the myofibroblasts. There are some differences between the small and large intestine in the magnitude of the reelin-Dab1 expression that might be a consequence of their homeostatic contribution to the different intestinal regions. Thus, the age-related changes in reelin-Dab1 expression are much smaller than those previously observed in rat small intestine [4] and Dab1 mRNA abundance is approx. 100 times greater in the small intestine than in the distal colon. The latter observation might indicate reelin-independent actions of Dab1 in the small intestine. The reelin detected in the muscle layer may correspond to that observed by Böttner et al. [19] in the enteric nerve plexuses, but they did not detect reelin expression in the myofibroblasts. They attributed these differences to the anti-reelin antibody they used for their study.

Since the first description of the reeler mouse some 60 years ago, the functions of reelin have been studied intensively in the central nervous system, but its role in peripheral tissues is not very well understood. The current observations reveal that the colon responds to DSS-treatment by increasing reelin production. The DSS-treatment also increases α-SMA expression that might result from an increase in the number of myofibroblasts as found in mice [20] and human [21] colon in response to IL-1β and TNF-α. Even though DSS-treatment would augment the number of myofibroblasts, the up-regulation of reelin expression is higher and temporally delayed when compared to α-SMA. This finding indicates that the increment in reelin abundance results from activation of reelin gene expression rather than from an increase in the number of myofibroblasts. Altogether, the observations reveal that reelin, though it is down-

regulated after birth, is up-regulated under pathological conditions and could be added to the list of extracellular matrix components secreted by the myofibroblasts in health and under inflammatory conditions. Reports showing up-regulation of reelin following tissue injury in several organs [22–29] proposed a role for reelin in tissue repair and our previous observations, revealing reelin involvement in the homeostasis of the small intestine epithelium [5], are consistent with this role.

Several genetic and epigenetic mechanisms regulate reelin gene expression (see Grayson et al. [30] for a review). The reelin promoter region contains recognition sites for the transcription factors Sp1 and Tbr1 [30] and both factors up-regulate reelin expression in brain [31]. Tbr1 requires its association with CASK to activate reelin transcription in brain [32] and up-regulation of CASK and reelin has been observed in human esophageal carcinoma [33]. The current data reveal that the transcriptional control of reelin gene expression in the distal colon differs from those described in brain and that in esophageal carcinoma. Thus, neither Tbr1, Sp1 nor CASK seem to mediate the DSS-induced up-regulation of reelin, because Tbr1 mRNA is undetected in either control or DSS-treated colon and the DSS treatment does not modify Sp1 mRNA abundance and decreases that of CASK. At the present time we cannot discern whether the decrease in CASK mRNA abundance contributes to reelin up-regulation. Balmaceda et al. [34] reported that ApoER2 down-regulates reelin expression in a human neuroblastoma cell line but the current study shows that DSS-treatment co-upregulates ApoER2 and reelin. In agreement with Balmaceda et al. [34], we have shown that reelin down-regulation is accompanied by an increase in ApoER2 mRNA levels in human colon adenocarcinoma tissue [6]. These contradictory findings might indicate that the cell signalling systems that respond to colitis challenge differ from those in cancer cells, so that in the former the global output of the signalling systems is the activation of reelin transcription whereas in cancer cells the output is the down-regulation of reelin expression.

Reelin expression is also regulated by epigenetic mechanisms such as methylation and histone deacetylation [30]. Several studies revealed that histone acetylation/deacetylation and DNA-methylation are connected [30,31,35–39]. The reelin promoter region is embedded in a large CpG island and in the brain, reelin gene activity is silent when the CpG island is heavily methylated [31,35]. Studies in neural tissues and in cultured neural cells have shown that reelin transcription increases when DNMT1 gene expression decreases [30]. In agreement with these observations we found that

the DSS-induced reelin up-regulation is accompanied by: i) decreased abundance of DNMT1 mRNA and protein expression and ii) hypo-methylation of that sequence of the reelin promoter region that binds DNMT1 [18]. These findings indicate that the DSS-related reduction in the DNMT1 expression hypo-methylates the reelin gene and hence activates reelin transcription.

DSS-induced colitis also increases the mRNA levels of the growth factors TGF-β1. TGF-β1 behaves as an anti-inflammatory cytokine and affects several myofibroblasts processes. These processes include: i) an increase in α-SMA gene expression in human intestinal myofibroblasts [40], ii) the differentiation of rat intestine [41] and lung [42] myofibroblasts and iii) the inhibition of DNMT1 expression in rat lung myofibroblasts [42]. In accordance with these reports and our current data, we postulate that TGF-β1 might: i) contribute to the observed increase in α-SMA expression and ii) up-regulate reelin synthesis by down-regulating DNMT1. Whether reelin expression, which accelerates epithelial cell proliferation and migration in the small intestine [5], contributes to the anti-inflammatory action of TGF-β1 deserves further investigation. The co-upregulation of reelin and TGF-β1 found in the current study does not agree with reports showing that TGF-β1 down-regulates reelin expression in esophagous cancer [43]. Again, the up-regulation of a regulatory factor, in this case TGF-β1, is accompanied by either activation (acute colitis) or repression (esophagous cancer) of reelin transcription. As previously stated, the varied expression of TGF-β1 might be due to differences in cell signalling that may be modified under different pathological conditions. In support of this view, there are reports indicating that the reelin gene is hyper-methylated in human colon adenocarcinoma, breast, gastric and pancreatic cancers [6,37–39], whereas reelin hypo-methylation occurs in response to colitis. These observations reinforce the role of myofibroblasts in the intestinal physiology and pathology.

Finally we examined the role of reelin in DSS-induced colon inflammation by using reeler mice and the results showed that all the inflammatory parameters tested and the mortality are greater in the reeler than in the wild type mice. These findings indicate that the mutation aggravates DSS-colitis and corroborates the hypothesis that reelin protects the animal from colitis development.

In conclusion, the current work reveals that the colon myofibroblasts express reelin, that DSS-colitis activates reelin expression via DNMT1-dependent hypo-

methylation of the reelin gene promoter region and iii) reelin protects from colitis development.

Acknowledgements

The work was supported by a Grant from the Junta de Andalucía (CTS 5884) and by an associated pre-doctoral grant to Carvajal AE. We thank Dr. R Rámirez and Dr. F Sánchez de Medina for their technical help. Immunohistochenistry images were obtained in the “Centro de Investigación Tecnología e Innovación de la Universidad de Sevilla” (CITIUS), Universidad de Sevilla.

References

[1] L.G. van der Flier, H. Clevers, Stem cells, self-renewal, and differentiation in the intestinal epithelium, Annu. Rev. Physiol. 71 (2009) 241–260. doi:10.1146/annurev.physiol.010908.163145.

[2] A. Andoh, S. Bamba, M. Brittan, Y. Fujiyama, N.A. Wright, Role of intestinal subepithelial myofibroblasts in inflammation and regenerative response in the gut, Pharmacol. Ther. 114 (2007) 94–106. doi:10.1016/j.pharmthera.2006.12.004.

[3] D.W. Powell, I. V Pinchuk, J.I. Saada, X. Chen, R.C. Mifflin, Mesenchymal cells of the intestinal lamina propria, Annu. Rev. Physiol. 73 (2011) 213–37. doi:10.1146/annurev.physiol.70.113006.100646.

[4] P. García-Miranda, M.J. Peral, A.A. Ilundain, Rat small intestine expresses the reelin-Disabled-1 signalling pathway, Exp. Physiol. 95 (2010) 498–507. doi:10.1113/expphysiol.2009.050682.

[5] P. García-Miranda, M.D. Vázquez-Carretero, P. Sesma, M.J. Peral, A.A. Ilundain, Reelin is involved in the crypt-villus unit homeostasis, Tissue Eng. Part A. 19 (2013) 188–98. doi:10.1089/ten.TEA.2012.0050.

[6] J.M. Serrano-Morales, M.D. Vazquez-Carretero, M.J. Peral, A.A. Ilundain, P. Garcia-Miranda, Reelin-Dab1 signaling system in human colorectal cancer, Mol Carcinog. (2016). doi:10.1002/mc.22527.

[7] P. García-Miranda, M.D. Vázquez-Carretero, G. Gutiérrez, M.J. Peral, A. Ilundáin, Lack of reelin modifies the gene expression in the small intestine of mice, J. Physiol. Biochem. 68 (2012) 205–18. doi:10.1007/s13105-011-0132-0.

[8] A.E. Carvajal, M.D. Vazquez-Carretero, M.L. Calonge, A.A. Ilundain, M.J. Peral, Colitis up-regulates reelin expression in the colon, J. Physiol. Biochem. 69 (2013) 670–671. <Go to ISI>://WOS:000364786400208.

[9] A.E. Carvajal, A. de los Santos, M.D. Vazquez-Carretero, M.J. Peral, A.A. Ilundain, M.L. Calonge, The colon of control and reeler mice in health and disease, Acta Physiol. 212 (2014) 90. <Go to ISI>://WOS:000342750000216.

[10] A.E. Carvajal, M.D. Vazquez-Carretero, M.J. Peral, A.A. Ilundain, M.L. Calonge, DSS-induced inflammation and regulation of reelin gene expression in mouse colon, Acta Physiol. 215 (2015) 97. <Go to ISI>://WOS:000364786400207.

[11] G. D'Arcangelo, G.G. Miao, S.C. Chen, H.D. Soares, J.I. Morgan, T. Curran, A protein related to extracellular matrix proteins deleted in the mouse mutant reeler,

Nature. 374 (1995) 719–723. doi:10.1038/374719a0.

[12] H.S. Cooper, S.N. Murthy, R.S. Shah, D.J. Sedergran, Clinicopathologic study of dextran sulfate sodium experimental murine colitis, Lab. Investig. 69 (1993) 238–49. http://www.ncbi.nlm.nih.gov/pubmed/8350599.

[13] K.J. Livak, T.D. Schmittgen, Analysis of Relative Gene Expression Data Using Real-Time Quantitative PCR and the $2^{-\Delta\Delta CT}$ Method, Methods. 25 (2001) 402–408. doi:10.1006/meth.2001.1262.

[14] M.M. Bradford, A rapid and sensitive method for the quantitation of microgram quantities of protein utilizing the principle of protein-dye binding, Anal. Biochem. 72 (1976) 248–254. doi:10.1016/0003-2697(76)90527-3.

[15] J. Kiernan, Staining theory, Histol. Histochem. Methods. (2008) 67–104. http://www.scionpublishing.com/shop/product_display.asp?mscssid=MT4RPERE43AA9JFUTGV2TEX8NTU67Q03&CurrencyID=2&ProductID=9781904842422.

[16] J.E. Krawisz, P. Sharon, W.F. Stenson, Quantitative assay for acute intestinal inflammation based on myeloperoxidase activity. Assessment of inflammation in rat and hamster models, Gastroenterology. 87 (1984) 1344–50. doi:S0016508584003036 [pii].

[17] K. Patterson, L. Molloy, W. Qu, S. Clark, DNA methylation: bisulphite modification and analysis, J. Vis. Exp. (2011) 1–9. doi:10.3791/3170.

[18] F. Matrisciano, P. Tueting, I. Dalal, B. Kadriu, D.R. Grayson, J.M. Davis, F. Nicoletti, A. Guidotti, Epigenetic modifications of GABAergic interneurons are associated with the schizophrenia-like phenotype induced by prenatal stress in mice, Neuropharmacology. 68 (2013) 184–194. doi:10.1016/j.neuropharm.2012.04.013.

[19] M. Böttner, P. Ghorbani, J. Harde, M. Barrenschee, I. Hellwig, I. Vogel, M. Ebsen, E. Förster, T. Wedel, Expression and regulation of reelin and its receptors in the enteric nervous system, Mol. Cell. Neurosci. 61C (2014) 23–33. doi:10.1016/j.mcn.2014.05.001.

[20] K. Suzuki, X. Sun, M. Nagata, T. Kawase, H. Yamaguchi, V. Sukumaran, Y. Kawauchi, H. Kawachi, T. Nishino, K. Watanabe, H. Yoneyama, H. Asakura, Analysis of intestinal fibrosis in chronic colitis in mice induced by dextran sulfate sodium, Pathol. Int. 61 (2011) 228–238. doi:10.1111/j.1440-1827.2011.02647.x.

[21] T.M. Jobson, C.K. Billington, I.P. Hall, Regulation of proliferation of human colonic subepithelial myofibroblasts by mediators important in intestinal inflammation, J.

Clin. Invest. 101 (1998) 2650–2657. doi:10.1172/JCI1876.

[22] S. Courtès, J. Vernerey, L. Pujadas, K. Magalon, H. Cremer, E. Soriano, P. Durbec, M. Cayre, Reelin controls progenitor cell migration in the healthy and pathological adult mouse brain, PLoS One. 6 (2011) e20430. doi:10.1371/journal.pone.0020430.

[23] D. Kobold, A. Grundmann, F. Piscaglia, C. Eisenbach, K. Neubauer, J. Steffgen, G. Ramadori, T. Knittel, Expression of reelin in hepatic stellate cells and during hepatic tissue repair: a novel marker for the differentiation of HSC from other liver myofibroblasts, J. Hepatol. 36 (2002) 607–13. doi:10.1016/S0168-8278(02)00050-8.

[24] A. Botella-López, E. de Madaria, R. Jover, R. Bataller, P. Sancho-Bru, A. Candela, A. Compañ, M. Pérez-Mateo, S. Martínez, J. Sáez-Valero, Reelin is overexpressed in the liver and plasma of bile duct ligated rats and its levels and glycosylation are altered in plasma of humans with cirrhosis, Int. J. Biochem. Cell Biol. 40 (2008) 766–775. doi:10.1016/j.biocel.2007.10.021.

[25] R. Panteri, J. Mey, N. Zhelyaznik, A. D'Altocolle, A. Del Fà, C. Gangitano, R. Marino, E. Lorenzetto, M. Buffelli, F. Keller, Reelin is transiently expressed in the peripheral nerve during development and is upregulated following nerve crush, Mol. Cell. Neurosci. 32 (2006) 133–42. doi:10.1016/j.mcn.2006.03.004.

[26] C. Pasten, J. Cerda, I. Jausoro, F.A. Court, A. Cáceres, M.P. Marzolo, ApoER2 and Reelin are expressed in regenerating peripheral nerve and regulate Schwann cell migration by activating the Rac1 GEF protein, Tiam1, Mol. Cell. Neurosci. 69 (2015) 1–11. doi:10.1016/j.mcn.2015.09.004.

[27] A. Magnani, L. Pattacini, L. Boiardi, B. Casali, C. Salvarani, Reelin levels are increased in synovial fluid of patients with rheumatoid arthritis, Clin. Exp. Rheumatol. 28 (2010) 546–548.

[28] J.S. Pulido, I. Sugaya, J. Comstock, K. Sugaya, Reelin expression is upregulated following ocular tissue injury, Graefes Arch. Clin. Exp. Ophthalmol. 245 (2007) 889–93. doi:10.1007/s00417-006-0458-4.

[29] A. Saeed, L. Barreto, S.G. Neogii, A. Loos, I. McFarlane, A. Aslam, Identification of novel genes in Hirschsprung disease pathway using whole genome expression study, J. Pediatr. Surg. 47 (2012) 303–7. doi:10.1016/j.jpedsurg.2011.11.017.

[30] D.R. Grayson, Y. Chen, E. Costa, E. Dong, A. Guidotti, M. Kundakovic, R.P. Sharma, The human reelin gene: Transcription factors (+), repressors (-) and the

methylation switch (+/-) in schizophrenia, Pharmacol. Ther. 111 (2006) 272–286. doi:10.1016/j.pharmthera.2005.01.007.

[31] Y. Chen, R.P. Sharma, R.H. Costa, E. Costa, D.R. Grayson, On the epigenetic regulation of the human reelin promoter, Nucleic Acids Res. 30 (2002) 2930–2939. doi:10.1093/nar/gkf401.

[32] Y.P. Hsueh, T.F. Wang, F.C. Yang, M. Sheng, Nuclear translocation and transcription regulation by the membrane-associated guanylate kinase CASK/LIN-2, Nature. 404 (2000) 298–302. doi:10.1038/35005118.

[33] Q. Wang, J. Lu, C. Yang, X. Wang, L. Cheng, G. Hu, Y. Sun, X. Zhang, M. Wu, Z. Liu, CASK and its target gene Reelin were co-upregulated in human esophageal carcinoma, Cancer Lett. 179 (2002) 71–77. doi:10.1016/S0304-3835(01)00846-1.

[34] V. Balmaceda, I. Cuchillo-Ibáñez, L. Pujadas, M.S. García-Ayllón, C.A. Saura, J. Nimpf, E. Soriano, J. Sáez-Valero, ApoER2 processing by presenilin-1 modulates reelin expression, FASEB J. 28 (2014) 1543–1554. doi:10.1096/fj.13-239350.

[35] C.P. Mitchell, Y. Chen, M. Kundakovic, E. Costa, D.R. Grayson, Histone deacetylase inhibitors decrease reelin promoter methylation in vitro, J. Neurochem. 93 (2005) 483–492. doi:10.1111/j.1471-4159.2005.03040.x.

[36] E. Dong, A. Guidotti, D.R. Grayson, E. Costa, Histone hyperacetylation induces demethylation of reelin and 67-kDa glutamic acid decarboxylase promoters, Proc. Natl. Acad. Sci. U. S. A. 104 (2007) 4676–4681. doi:10.1073/pnas.0700529104.

[37] N. Sato, N. Fukushima, R. Chang, H. Matsubayashi, M. Goggins, Differential and epigenetic gene expression profiling identifies frequent disruption of the RELN pathway in pancreatic cancers, Gastroenterology. 130 (2006) 548–65. doi:10.1053/j.gastro.2005.11.008.

[38] O. Dohi, H. Takada, N. Wakabayashi, K. Yasui, C. Sakakura, S. Mitsufuji, Y. Naito, M. Taniwaki, T. Yoshikawa, Epigenetic silencing of RELN in gastric cancer, Int. J. Oncol. 36 (2010) 85–92. doi:10.3892/ijo.

[39] T. Stein, E. Cosimo, X. Yu, P.R. Smith, R. Simon, L. Cottrell, M.-A. Pringle, A.K. Bell, L. Lattanzio, G. Sauter, C. Lo Nigro, T. Crook, L.M. Machesky, B.A. Gusterson, Loss of reelin expression in breast cancer is epigenetically controlled and associated with poor prognosis, Am. J. Pathol. 177 (2010) 2323–33. doi:10.2353/ajpath.2010.100209.

[40] C. Francoeur, Y. Bouatrouss, A. Seltana, I. V. Pinchuk, P.H. Vachon, D.W. Powell, B. Sawan, E.G. Seidman, J.F. Beaulieu, Degeneration of the Pericryptal

Myofibroblast Sheath by Proinflammatory Cytokines in Inflammatory Bowel Diseases, Gastroenterology. 136 (2009). doi:10.1053/j.gastro.2008.10.014.

[41] J.G. Simmons, J.B. Pucilowska, T.O. Keku, P.K. Lund, IGF-I and TGF-beta1 have distinct effects on phenotype and proliferation of intestinal fibroblasts, Am. J. Physiol. Gastrointest. Liver Physiol. 283 (2002) G809-18. doi:10.1152/ajpgi.00057.2002.

[42] B. Hu, M. Gharaee-Kermani, Z. Wu, S.H. Phan, Epigenetic regulation of myofibroblast differentiation by DNA methylation, Am. J. Pathol. 177 (2010) 21–28. doi:10.2353/ajpath.2010.090999.

[43] Y. Yuan, H. Chen, G. Ma, X. Cao, Z. Liu, Reelin is involved in transforming growth factor-β1-induced cell migration in esophageal carcinoma cells, PLoS One. 7 (2012) e31802. doi:10.1371/journal.pone.0031802.

Legends

Fig. 1. Reelin and Dab1 mRNA abundance along the mouse intestine. RT-PCR was performed on total RNA isolated from duodenum, jejunum, ileum, proximal colon and distal colon of 3 month-old mice. Data were normalized to β-actin. The Dab1 mRNA levels measured in distal colon were set at 1. The histograms represent the means ± SEM of arbitrary units of mRNA abundance and are plotted on a logarithmic scale. The number of animals was 5. One-way Anova showed an effect of intestinal region on Dab1 expression ($p<0.001$). Newman–Keul's test: $^{\#}p<0.001$ intestinal region *vs*. jejunum.

Fig. 2. Reelin and Dab1 mRNA expression in proximal and distal colon *vs*. age. 16 day-, 30 day- and 90 day-old mice were used. Data were normalized to β-actin. The Dab1 mRNA levels measured in the distal colon of 3 month-old mice were set at 1. Means ± SEM of arbitrary units of mRNA abundance are plotted *vs*. age. The number of animals for each age was 5. One-way Anova showed an effect of age on reelin expression ($p<0.001$). Newman–Keul's test: $^{*}p<0.001$ *vs*. 16 day-old; $^{\#}p<0.001$ distal colon *vs*. proximal colon.

Fig. 3. Immunolocalization of Reelin, Dab1, VLDLR and ApoER2 in colon. 7 µm distal colon sections (T) were incubated with either anti-reelin G10 (1:100 dilution), anti-Dab1 (1:200 dilution), anti-VLDLR (1:50 dilution), anti-ApoER2 (1:50 dilution) or anti-α-SMA (1:200 dilution) antibodies. Antibody binding was visualized with FITC-conjugated anti-rabbit IgG, FITC-conjugated anti-mouse IgG or Alexa Fluor 546 anti-mouse IgG (red). Nuclei were visualized with Hoechst. Scale bars represent 50 µm. Colonocytes and myofibroblasts were obtained from the colon of 90 day-old mice. Isolated colonocytes (C) and myofibroblasts (M) were immunostained with antibodies raised either against reelin sc5578 (1:50 dilution), Dab1 (1:200 dilution), VLDLR (1:25 dilution), ApoER2 (1:25 dilution) or anti-α-SMA (1:100 dilution). Antibody binding was visualized with biotinylated secondary antibodies. α-SMA was used as a myofibroblasts marker. Scale bar=10 µm. Negative controls without primary antibody were run in parallel. The photographs are representative of three different assays.

Fig. 4. Evaluation of the DSS-induced colitis. 3% DSS (dextran sulphate sodium) was administered in the drinking water during 9 days as described in Methods. The DAI (disease activity index) was assessed daily. The inflammatory indicators evaluated at the end of the treatment are: representative photographs of large intestine and cecum, colon weight/length ratio, MPO (myeloperoxidase) activity, mRNA relative abundance of IL-1β and TNF-α and representative H&E stained colon sections. The IL-1β mRNA levels measured in the proximal colon of control mice were set at 1. Data are means ± SEM. The number of animals was 10 for each experimental condition. PC: proximal colon, DC: distal colon, M: mucosa, ML: muscle layer. Student's t-test: *p<0.001 DSS-treated *vs*. untreated colon, $^{\#}$p<0.001 distal *vs.* proximal colon. Scale bar = 100 µm.

Fig. 5. DSS-induced colitis and the mRNA abundance of the reelin signalling system. The proximal and distal colon of 90 day-old mice were used. The histograms represent the means ± SEM of mRNA abundance fold change produced by DSS treatment relative to control mice. Dashed line represents a fold change value of 1. The number of animals was 10 for each condition. One-way Anova showed an effect of the DSS-treatment on the colon (p<0.001). Newman–Keul's test: ^{a}p<0.001 *vs*. α-SMA change, ^{b}p<0.001 distal *vs*. proximal colon. *p<0.001, $^{\#}$p<0.05, DSS-treated *vs*. untreated colon.

Fig. 6. Reelin and α-SMA mRNA levels in the distal colon of mice treated with DSS during either 0, 3, 6 or 9 days. The distal colon of 3 month-old mice was used. The following parameters are displayed: DAI (disease activity index), histological score of colon mice and mRNA relative abundance of IL-1β, TNF-α, reelin and α-SMA. The IL-1β and reelin mRNA levels measured at 0 days were set at 1. The number of animals used in each experimental condition was 9. Others details as in Figure 1. Student's t-test: *p<0.001, $^{\#}$p<0.05, DSS-treated *vs*. untreated colon.

Fig. 7. Western assays of reelin and α-SMA in the distal colon of mice treated with DSS during 0, 3, 6 and 9 days. 50 µg protein from either intact colon, mucosa or muscle layer of control and DSS-treated 3 month-old mice were loaded in each lane. Protein was also extracted from the intact colon of wild-type and reeler mice. The blots were probed with either anti-reelin G10 (1:500) or anti-α-SMA (1:10,000) antibodies, as described in the Methods. The blot is representative of three assays. Histograms represent the relative abundance of full-length reelin and of α-SMA normalized with either anti-β-actin

(1:4,000) or anti-GADPH (1:15,000), respectively. Values are means ± SEM, n =3. One-way Anova showed an effect of the duration of DSS-treatment on the gene studied ($p<0.001$). Newman–Keul's test: *$p<0.001$, 3, 6 or 9 days of treatment *vs.* 0 days treatment; [a]$p<0.001$, 6 or 9 days *vs.* 3 days of treatment; [b]$p<0.001$, 9 days *vs.* 6 days ; [c]$p<0.001$, muscle layer *vs.* mucosa.

Fig. 8. Regulation of reelin gene expression. Distal colon of 3 month-old mice with or without DSS-treatment was used. A, mRNA levels of CASK, Sp1, DNMT1, TGF-β1 and PDGF-BB. The ApoER2 mRNA values given in the present Figure are those shown as fold change in Figure 5. The ApoER2 mRNA levels measured in control mice were set at 1. The number of animals was 5. B, Western blot of DNMT1. 50 µg protein extracted from either the untreated or DSS-treated colon were loaded in each lane and the anti-DNMT1 antibody (1:4,000) was probed as described in Methods. The blot is representative of three assays. Histograms represent the relative abundance of DNMT1 normalized with β-actin. Values are means ± SEM. Student's t-test *$p<0.001$, DSS-treated *vs*. untreated colon.

Fig. 9. DSS-treatment and methylation levels of reelin promoter. Genomic DNA was isolated from distal colon of either control or 3% DSS-treated 3 month-old mice. The duration of the treatment was 9 days. The DNA was treated with sodium bisulfite as described in Methods. PCR primers were used to amplify the DNMT1 binding sequence of the reelin promoter region and the DNA extracted was sequenced by the Genomics and Sequence Service (IBIS, Seville). Five mice of each condition were used. Results are expressed as % of 5´CpG methylation *vs.* their position in the reelin promoter region. Values are means ± SEM Student's t-test: **$p<0.001$, *$p<0.01$, DSS-treated *vs.* untreated animals.

Fig. 10. Evaluation of the DSS induced inflammation in control and *reeler mice*

Mice of 3 month-old were subjected to 3 % dextran sulfate sodium (DSS) in the drinking water for up to 9 days. The microphotographs are representative of 6 different assays performed on 6 reeler and 6 control mice. One-way ANOVA showed an effect of mutation and of inflammation on DAI, ($p<0.01$) and distal colon ($p<0.05$). Newman–Keuls' test: *$p < 0.01$ and **$p < 0.05$ *reeler vs.* control mice

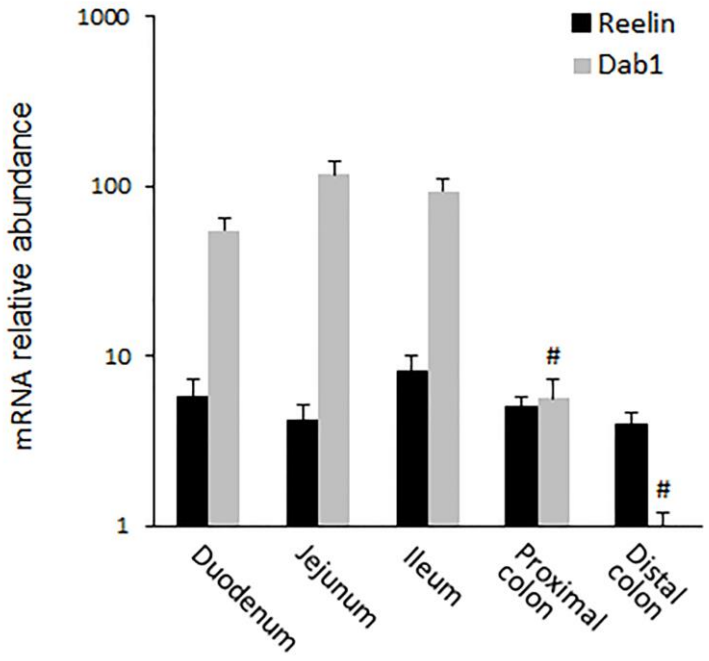
Reelin
Dab1
mRNA relative abundance
1000
100
10
1
#
#
Duodenum
Jejunum
Ileum
Proximal colon
Distal colon

Fig. 1

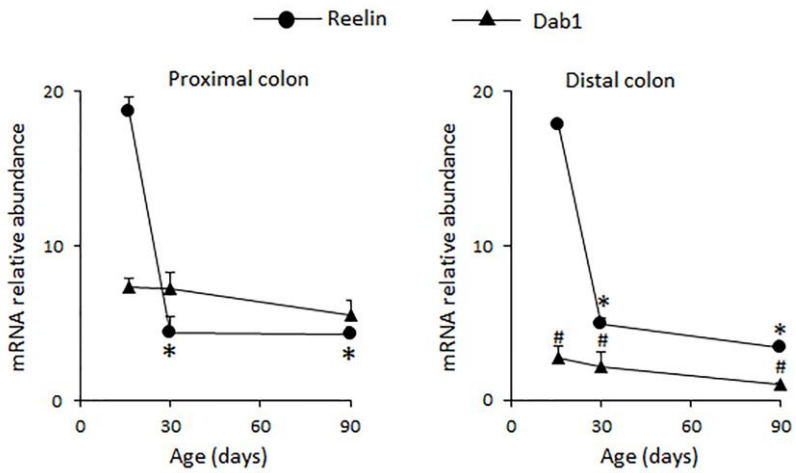
Reelin
Dab1
Proximal colon
Distal colon
mRNA relative abundance
Age (days)
0
10
20
30
60
90
*
#

Fig. 2

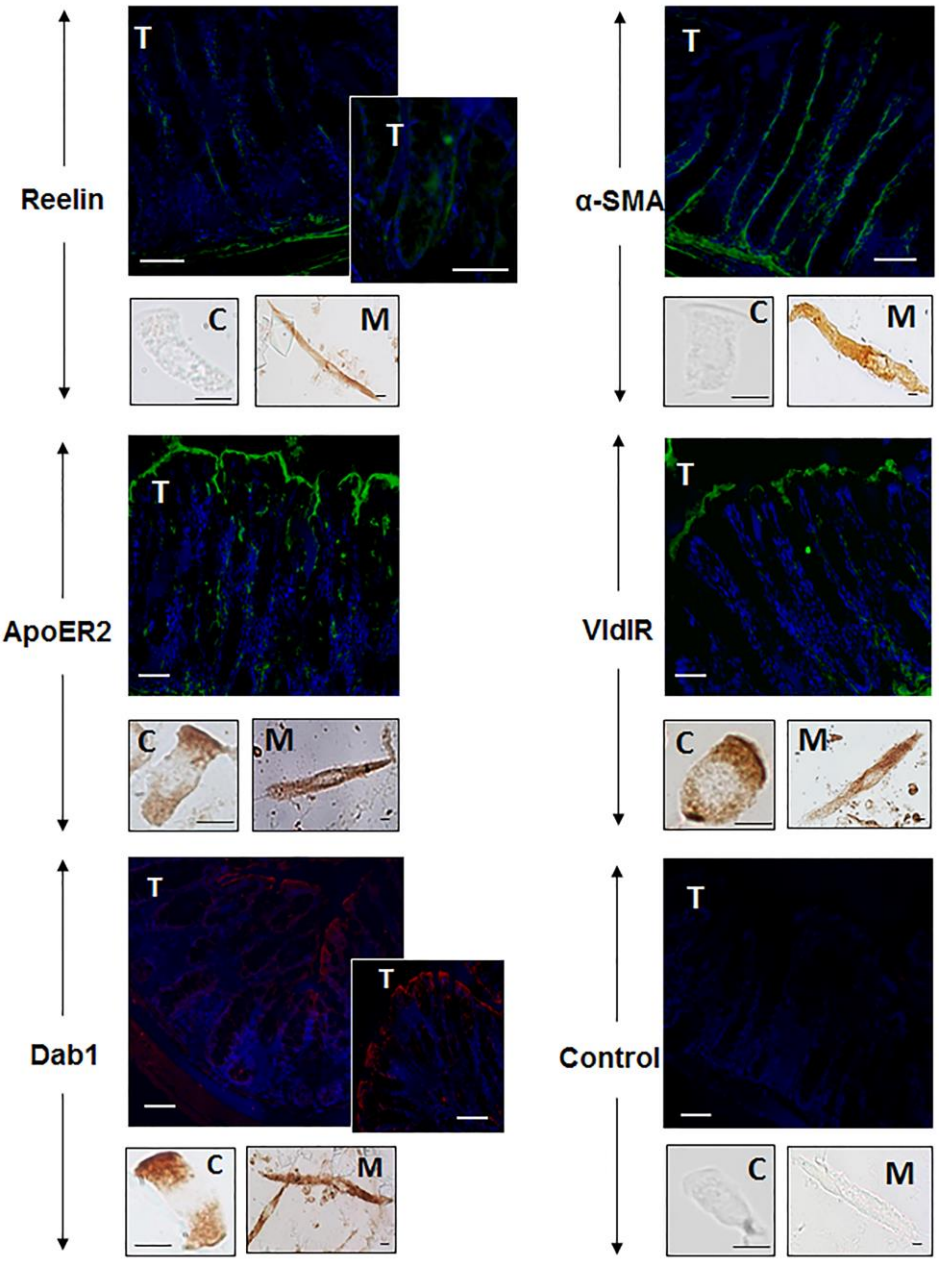
Reelin
T
T
C
M
α-SMA
T
C
M
ApoER2
T
C
M
VldlR
T
C
M
Dab1
T
T
C
M
Control
T
C
M

Fig. 3

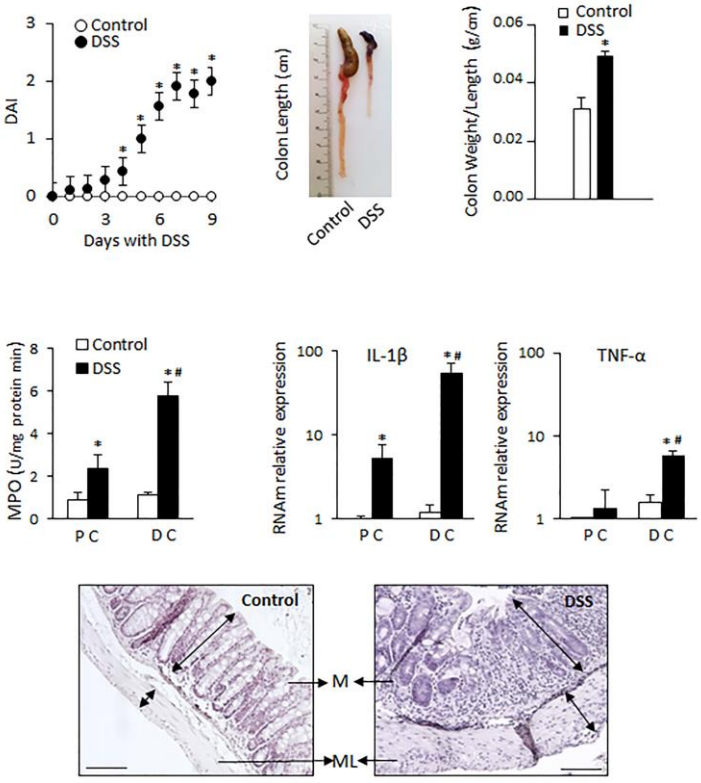
Control
DSS
DAI
Days with DSS
Colon Length (cm)
Control
DSS
Colon Weight/Length (g/cm)
MPO (U/mg protein min)
RNAm relative expression
IL-1β
TNF-α
P C
D C
Control
DSS
M
ML

Fig. 4

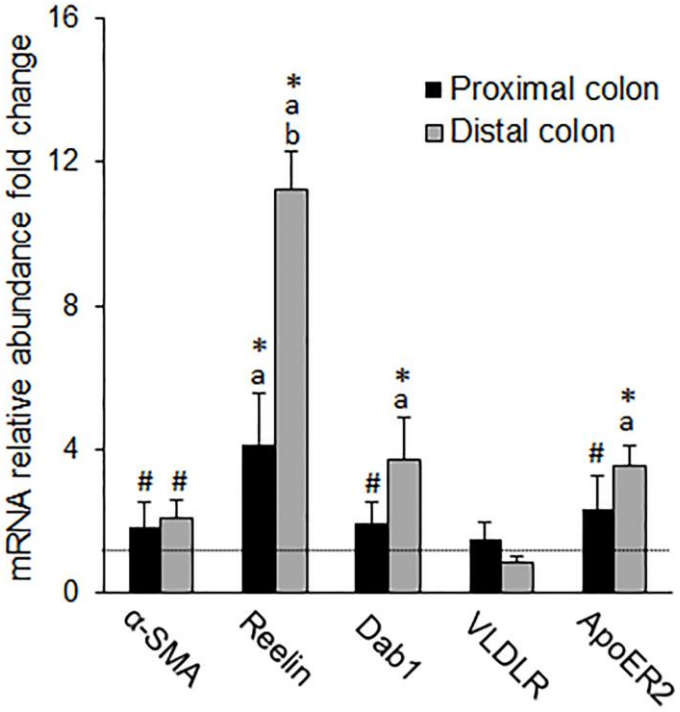
mRNA relative abundance fold change
16
12
8
4
0
Proximal colon
Distal colon
α-SMA
Reelin
Dab1
VLDLR
ApoER2

Fig. 5

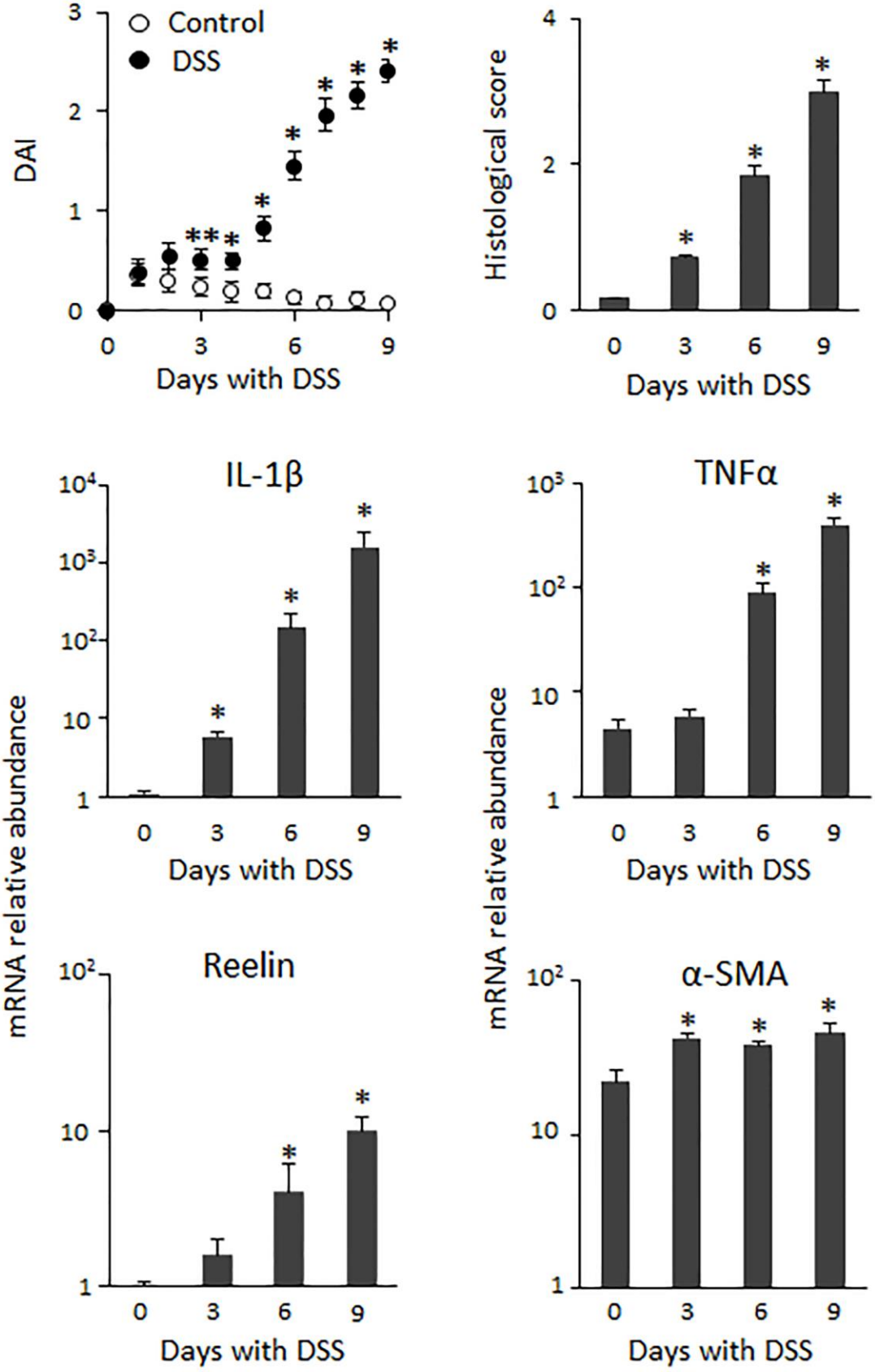
Control
DSS
DAI
Days with DSS
Histological score
Days with DSS
IL-1β
mRNA relative abundance
Days with DSS
TNFα
mRNA relative abundance
Days with DSS
Reelin
Days with DSS
α-SMA
Days with DSS

Fig. 6

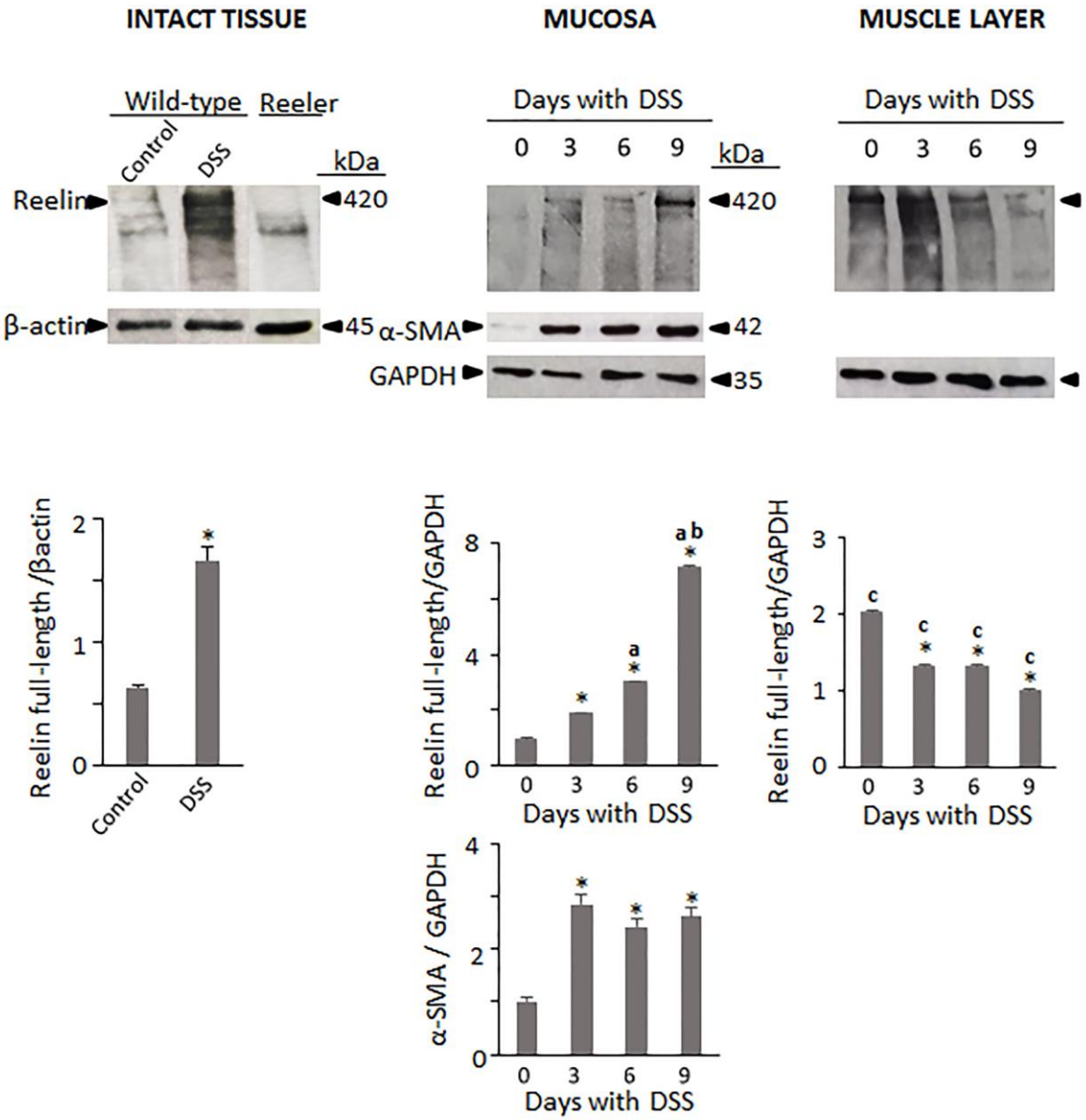
INTACT TISSUE
MUCOSA
MUSCLE LAYER
Wild-type
Reeler
Control
DSS
kDa
Reelin
420
β-actin
45
Days with DSS
0 3 6 9
kDa
420
α-SMA
42
GAPDH
35
Days with DSS
0 3 6 9
Reelin full-length /βactin
Control
DSS
Reelin full-length/GAPDH
Days with DSS
a b
a
Reelin full-length/GAPDH
Days with DSS
c
α-SMA / GAPDH
Days with DSS

Fig. 7

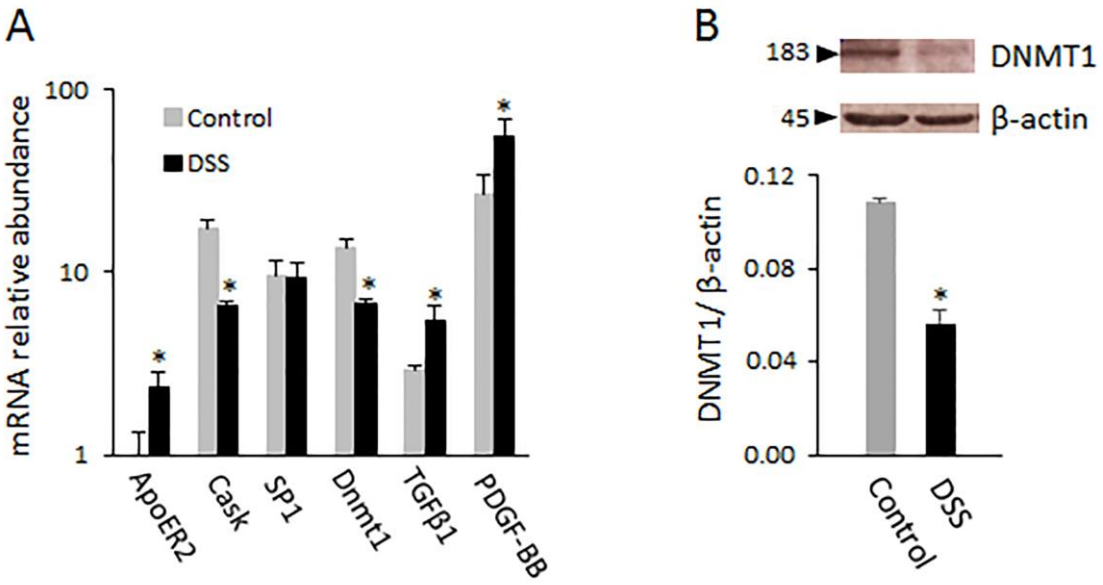
A
mRNA relative abundance
100
10
1
Control
DSS
ApoER2
Cask
SP1
Dnmt1
TGFβ1
PDGF-BB
B
183
DNMT1
45
β-actin
DNMT1/ β-actin
0.12
0.08
0.04
0.00
Control
DSS

Fig. 8

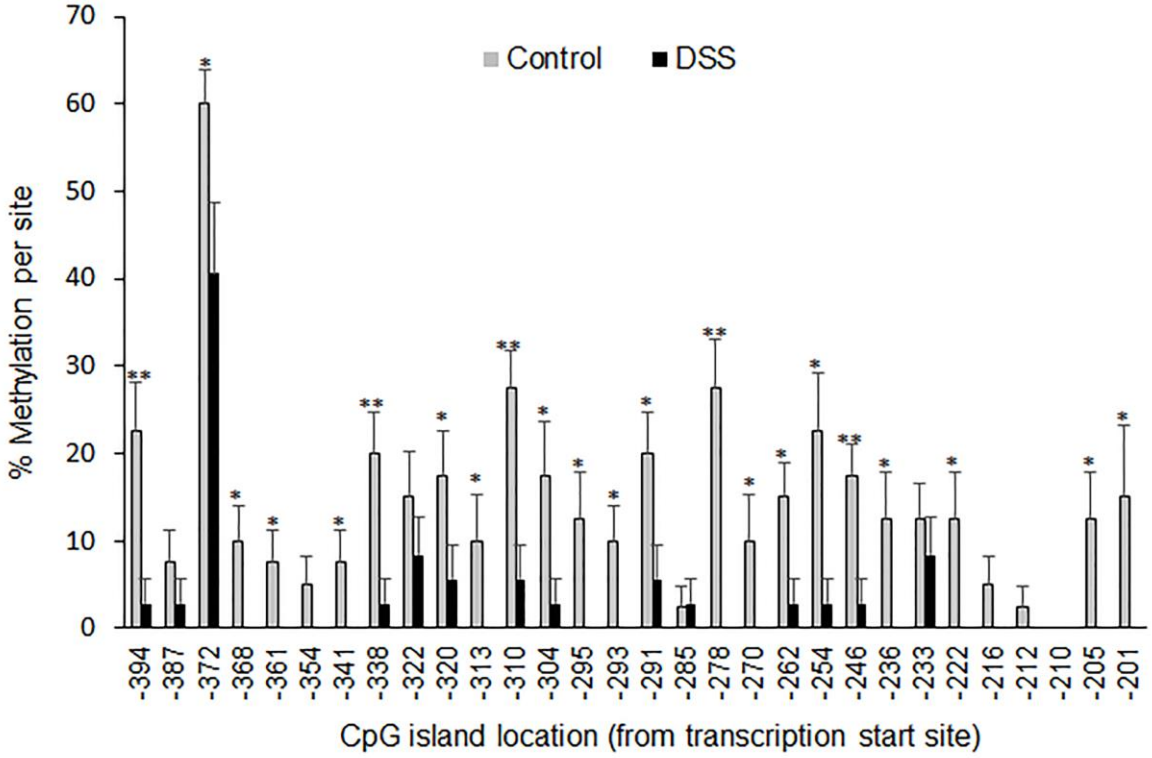
70
60
50
40
30
20
10
0
% Methylation per site
Control
DSS
-394
-387
-372
-368
-361
-354
-341
-338
-322
-320
-313
-310
-304
-295
-293
-291
-285
-278
-270
-262
-254
-246
-236
-233
-222
-216
-212
-210
-205
-201
CpG island location (from transcription start site)

Fig. 9